Electrostatic Penetration Effects Stand at the Heart of Aromatic π Interactions

Enrique M. Cabaleiro-Lago,[*,a] Jesús Rodríguez-Otero[*,b], Saulo A. Vázquez[b]

a. Facultade de Ciencias (Dpto. de Química Física), Universidade de Santiago de Compostela, Campus de Lugo. Avda. Alfonso X El Sabio s/n 27002 Lugo, Galicia (Spain).

b. Facultade de Química (Dpto. de Química Física), Universidade de Santiago de Compostela, 15782 Santiago de Compostela, Galicia (Spain).

Abstract

The nature of the interaction in benzene-containing dimers has been analysed by means of Symmetry Adapted Perturbation Theory (SAPT). The total interaction energy and the preference for the dimers to adopt slipped structures are, apparently, consequence of the balance between repulsion and dispersion. However, our results indicate that this only holds when trends are analysed using fixed intermolecular distances. Employing the most favourable separations between rings it turns out that the changes on the total interaction energy are mostly controlled by electrostatics, while repulsion and dispersion cancel each other to a great extent. Most of the electrostatic contribution is accounted for by electrostatic penetration, so a description based on multipoles should not be employed to rationalise the interaction in benzene-containing dimers. The changes on the interaction energy in benzene-containing dimers are steered by electrostatic penetration which, though often overlooked, plays an essential role for the description of aromatic π interactions.

1. Introduction

The interaction between aromatic rings has been recognized as one of the key interacting motifs in different systems, ranging from proteins to fullerenes.[1-5] Despite having been studied for quite a long time, especially for the prototypical benzene dimer, in recent years there has been a renewed interest in the characteristics of the interactions involving aromatic systems and the factors controlling them.

The focus of these recent studies has been to elucidate whether there exists an aromatic stacking interaction with particular or special properties when compared to other interacting arrangements.[6-11] Different studies have shown that probably there is not such a special stacking aromatic interaction except in the case when extended aromatic systems are involved.[7, 11] In fact, it has been proposed that the term π-π stacking interaction should be employed just as a geometry descriptor without implications as to its characteristics and strength.[12] Also, there has been substantial debate regarding the nature of the interaction, though dispersion is usually the largest contribution to the stability of stacked complexes.[7, 11, 13-15] However, the observed behaviour can be altered upon substitution or geometry changes and, even though the dispersion term could be the largest contribution, the changes in interaction strength upon substitution can be controlled by electrostatics.[16]

Benzene dimer has several minima, with the stacked parallel-displaced minimum reaching a stabilisation of -2.7 kcal mol^{-1}, though a T-shaped structure driven by C-H···π contacts is slightly more stable (-2.8 kcal mol^{-1}).[13-15, 17-21] The stabilization is controlled by dispersion and electrostatics, amounting to -4.5 and -1.6 kcal mol^{-1} in the T-shaped structure and to -6.6 and -1.4 kcal mol^{-1} in the parallel-displaced one, respectively.[11, 13] Hunter and Saunders proposed a simple model, based on the interaction between benzene quadrupole moments, to explain the most favourable orientations for benzene dimer, as well as the preferences in the interaction between electron-rich and electron-deficient aromatic systems.[22, 23] However, evidence has accumulated pointing to deviations from this simple model. Sherrill et al. showed that the interaction between substituted aromatic rings increased compared with benzene dimer unregards of the electron-withdrawing or electron-donor character of the substituent.[24-26] Also, Wheeler and Houk proposed a new model that considers that the observed substituent effect is due to direct through-space interactions between the substituent and the other molecule.[27-30] Thus, it does not matter whether the substituent is electron-withdrawing or electron-donor, but how it interacts directly with the other aromatic ring.

Very recently, Carter-Fenk and Herbert have proposed that the very nature of aromatic π interactions should be reconsidered,[31, 32] because the most favourable geometric arrangements (slipped structures in benzene dimer) are not the result of a balance between electrostatics and dispersion but a consequence of the interplay between dispersion and Pauli repulsion. These authors proposed a model that is capable of reproducing the geometrical preferences of different aromatic dimers without an

explicit electrostatic term and based only on van der Waals (dispersion and repulsion) contributions. However, this is in conflict with other authors who emphasized the crucial role of electrostatics in π interactions.[13, 14, 16, 19, 33] Ninkovic et al. recently showed that it is precisely electrostatics the contribution making the difference when comparing aromatic and non-aromatic stacking interactions.[19] Comparing benzene dimer and cyclohexane-benzene dimer, these authors showed that the main difference between them is that the interaction in benzene dimer is more long-ranged, essentially as a consequence of electrostatics. Thus, there is some disagreement as to the role played by electrostatics in aromatic interactions and whether it is a crucial contribution or it simply does not play a role determining the most stable geometrical arrangements.

Even though it is quite common to resort to multipole interactions (dipole-dipole, quadrupole-quadrupole, etc.) to rationalize the characteristics of dimers, their use should be taken with care, because the multipole expansion does not hold at the distances usually found in the minimum-energy structures.[34] The difference between the quantum-chemically computed electrostatic energy and the one obtained from a multipole expansion is called the electrostatic penetration energy. Its contribution can be crucial in the region of the minima where charge overlap can be significant and therefore the multipole expansion does not hold. Results obtained by other authors emphasize the role of electrostatic penetration effects: Ryno et al. observed that electrostatic penetration effects can amount to 50% of the total interaction energy in linear acene dimers,[33] while the results obtained by Gryn'ova et al. highlight the relevance of penetration effects on hydrocarbon dimers[35] Also, different studies have already shown that the electrostatic interaction in benzene dimers is in fact attractive even for the sandwich structure where the quadrupolar interaction must be repulsive[14, 16, 18, 20] and, very recently, Herbert has collected a series of examples where the use of a electrostatic energy based on multipoles leads to misleading interpretations and wrong results.[36] Thus, models based on a multipolar description of electrostatics will lack the contribution from electrostatic penetration at short distances and should be corrected accordingly by including an electrostatic penetration term or, more frequently, by including the penetration effects into the van der Waals terms.[37-40]

In the present work, a thorough exploration of the potential energy surface of benzene-containing dimers is performed, analysing the contributions that dominate the interaction in order to shed light on the role electrostatics plays in the interaction involving aromatic species. It will be shown that the electrostatic contribution plays a dominant role in determining the most stable structures of the dimers, though its contribution mainly comes from penetration effects.

2. Computational Details

The dimers studied are summarized in Figure 1, and correspond to systems formed by one benzene molecule and another aromatic species among benzene, trifluorobenzene, triazine, borazine, and hexafluorobenzene, which have been selected for being nonpolar while showing a variety of quadrupole moments; therefore, they should lead to different electrostatic interactions if the simple multipole picture applies. Besides, the dimer formed by benzene and cyclohexane has been included to provide a comparison between the characteristics of π-π and σ-π stacking interactions.

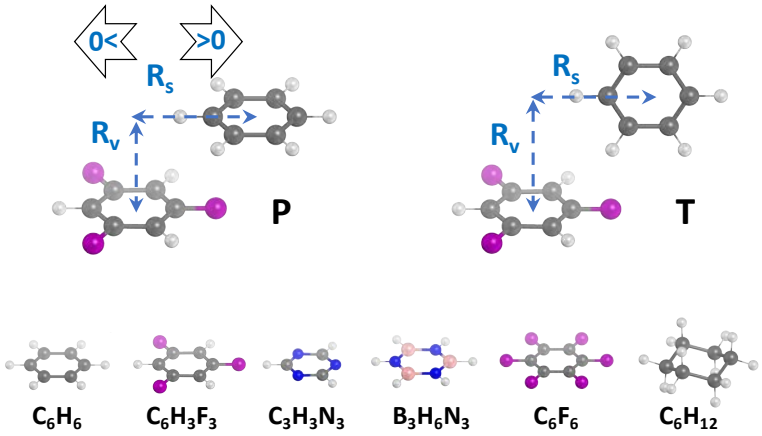

Figure 1. Systems considered in this work: parallel and T-shaped dimers formed by benzene, trifluorobenzene, triazine, borazine, hexafluorobenzene and cyclohexane (parallel only) with benzene. The intermolecular geometry is modified by changing R_v and R_s.

Figure 1 shows the structures employed for studying the potential energy surfaces of the dimers, corresponding to a prototypical parallel stacked dimer (P) and to a tilted T-shaped structure (T) similar to that found in the herringbone pattern observed in benzene crystal.[41] Two-dimensional scans were performed by changing the vertical displacement between ring centres (R_v in Figure 1) and the lateral displacement (R_s in Figure 1) controlling the parallel shift of the rings. R_v has been changed in 0.10 Å increments spanning a range of 4 Å, while the rings were slipped in 0.25 Å increments between -5 and 5 Å from the ring centre. The characteristics of the interaction are then analysed at a fixed interplane distance (constant R_v), but also by computing the most favourable vertical displacement for a given parallel displacement, obtained by interpolation of the energy values at different R_v for a given R_s. This is important because using a fixed R_v the dimers can move into quite repulsive regions when approaching the sandwich position, so the results could be significantly different from those obtained following the most favourable vertical displacements.

Interaction energies for all dimers have been obtained by using a symmetry adapted perturbation theory (SAPT) method together with the jun-cc-pVDZ basis set.[42, 43] As already shown by Parker et al., this level of calculation provides results similar to those obtained with higher levels of SAPT at a reduced computational cost.[44] Also, in a previous work of the authors on benzene dimer, the results obtained with SAPT0/jun-cc-pVDZ where pretty similar to those found at the SAPT2+(3) δMP_2/aug-cc-pVTZ.[16] Thus, considering the large amount of calculations at different geometries that need to be performed, the cheaper SAPT0/jun-cc-pVDZ level has been employed throughout. This simplest SAPT level, SAPT0, is obtained by including the following terms:

$$E_{SAPT0} = E^{10}_{electr} + E^{10}_{exch} + E^{20}_{ind} + E^{20}_{exch,ind} + E^{20}_{disp} + E^{20}_{exch,disp} + \delta HF$$

with δHF being a term trying to represent induction to higher orders. The contributions are usually grouped as follows: $E_{ele} = E^{10}_{electr}$; $E_{rep} = E^{10}_{exch}$; $E_{ind} = E^{20}_{exch,ind} + E^{20}_{ind} + \delta HF$; $E_{dis} = E^{20}_{exch,dis} + E^{20}_{dis}$, corresponding to electrostatic, repulsion, induction and dispersion contributions to the interaction energy. A further grouping can also be done by collecting electrostatic ($E_{ele+ind} = E_{ele} + E_{ind}$) and non-electrostatic terms ($E_{rep+dis} = E_{rep} + E_{dis}$), facilitating their comparison since, quite commonly, repulsion and dispersion somewhat cancel each other near the minima.

The electrostatic contribution E_{ele} has been further divided into multipolar (E_{DMA}) and penetration (E_{pen}) energies.[34] To obtain the multipolar electrostatic energy, a Distributed Multipole Analysis (DMA) is employed with multipoles obtained at the HF/jun-cc-pVDZ level, which is the same level employed in SAPT0 calculations.[34, 45] Multipoles are distributed over all atoms in a given molecule, reaching up to rank 4 (hexadecapole) for heavy atoms and to rank 2 (quadrupole) for hydrogen atoms. These multipoles should provide an almost exact representation of electrostatics at long range, avoiding convergence problems as the intermolecular distances shorten. The contribution of electrostatic penetration is obtained at each geometry as the difference between the electrostatic energy obtained by SAPT0 and the multipolar electrostatic energy; $E_{pen} = E_{ele} - E_{DMA}$.

Monomer geometries have been obtained at the B3LYP/def2-TZVPP level by using Turbomole 6.3 and imposing symmetry restrictions.[46] The multipolar electrostatic energy was obtained employing Orient,[47] with multipole moments computed with GDMA[45] using wavefunctions for the monomers obtained with Gaussian16.[48] All SAPT0 calculations have been performed with the PSI4 program.[49]

3. Results

3.1. Benzene dimer

In this section a thorough exploration of the characteristics of the potential energy surface of the benzene dimer is presented and discussed. As indicated above, one molecule is kept fixed with its centre at the origin while the second molecule is located

at different lateral displacements along an axis passing through two *para* carbon atoms. For each lateral displacement R_s, potential energy curves were obtained at different vertical separations (R_v) between ring centres for the two orientations (P and T) shown in Figure 1. A different T-shaped structure has been considered, but since it shows very similar results it is included in the Supplementary Information (Figure S1).

Previous work has already shown that for the parallel-displaced structure, the minimum corresponds to a vertical distance between ring planes of around 3.5-3.6 Å.[13, 18, 20, 21] Similarly, for the T-shaped structure shown in Figure 1, the minimum is located at vertical distances of around 4.9 Å.[18, 20, 21] The analysis is first carried out by changing only one variable, namely R_s, while keeping R_v at a value of 3.6 Å and 4.9 Å, close to the optimum value for P and T structures, respectively. Figure 2 shows the results obtained under these conditions for the interaction energy and its different SAPT0 contributions.

Considering the parallel structure, it is clearly shown in Figure 2 (left, top) that the most stable structure corresponds to a slipped geometry. The potential energy curve shows two equivalent minima at a lateral displacement of around 1.5 Å, while a maximum is observed for the sandwich structure (R_s = 0). The largest stabilising contribution to the interaction energy in benzene dimer is dispersion, partially cancelled out by large repulsion contributions. Dispersion favours the sandwich structure, where its contribution is maximum, while repulsion has the contrary effect, penalising structures with small lateral displacement. On the other hand, the quite small electrostatic contribution shows a minimum for zero displacement and therefore could not be the origin of the preference for slipped structures. While induction slightly favours the slipped structure, its contribution is too small to have a real impact on the final energetics of the system. In the case of the T-shaped structure, the overall behaviour is quite similar. The interaction energy also shows a double well of similar magnitude as those obtained for parallel-slipped structures. However, even though the total interaction energies are similar in both structures, the contributions from dispersion and repulsion are significantly smaller due to the larger distances between atoms in the T-shaped structure. In any case, dispersion favours the structure with no horizontal displacement (R_s = 0) while repulsion hinders it. The electrostatic contribution is larger than in parallel structures due to the presence of C-H···π contacts, and a similar enhancement is observed for induction, though none of these contributions favour the slipped structure.

These results are similar to others found in literature, with dispersion dominating the stabilization of the dimer.[13-15] In any case, none of the stabilising contributions favour the formation of the slipped structure, and only repulsion favours its formation by penalising the non-displaced arrangement. Thus, the results would indicate that it is the repulsion term the one forcing benzene dimer to adopt a slipped structure while electrostatics play no role. Based on this behaviour, Carter-Fenk and Herbert proposed that the position of the minimum in benzene dimer and other aromatic species can be

described by a balance between dispersion and repulsion, with no role played by electrostatics.[31, 32] This is more clearly seen when considering electrostatic ($E_{ele+ind}$) and non-electrostatic ($E_{rep+dis}$) grouped contributions (Figure 2, right). It can be observed that in both P and T structures the $E_{ele+ind}$ energy shows a minimum at zero displacement while the $E_{rep+dis}$ term shows minima at the slipped structures. It becomes clear from Figure 2 that the total interaction energy curve roughly follows the behaviour of the combined $E_{rep+dis}$ contribution, while the $E_{ele+ind}$ contribution just adds to the total stability of the dimer.

Figure 2 also shows that the electrostatic term mostly comes from penetration, while the multipolar contribution changes in a totally different way, with a clear maximum in the parallel sandwich structure and a minimum for zero displacement in the T dimer. Thus, trying to rationalize the contribution from electrostatics by simple multipole models can lead to totally misleading conclusions. According to multipoles, the parallel structure is electrostatically repulsive, while SAPT0 indicates that it really is attractive. As indicated above, no analysis about electrostatics should be done employing a multipolar approach for distances near the minima.

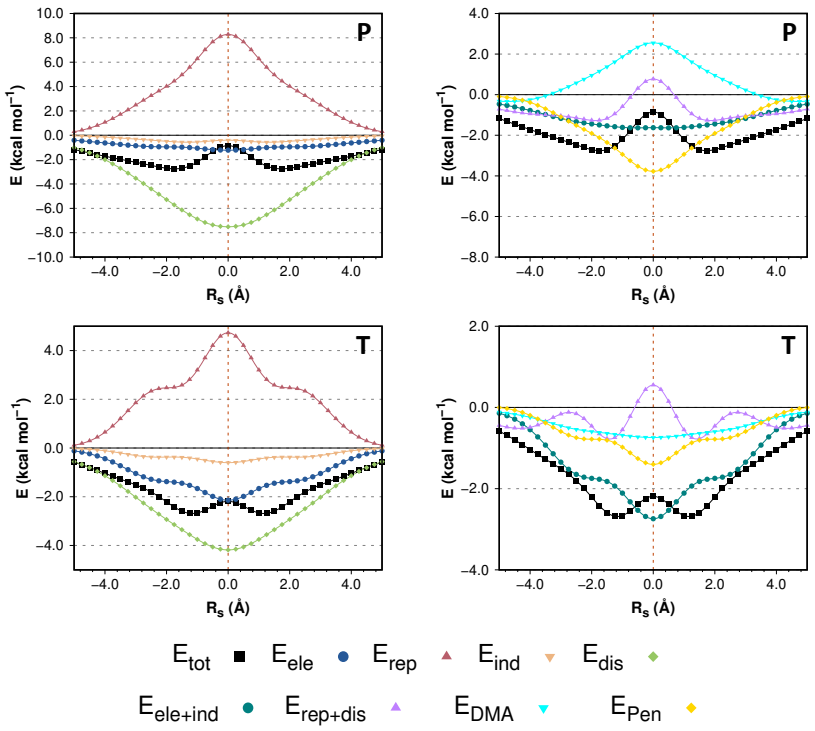

Figure 2. Potential energy curves for benzene dimer as obtained with SAPT0/jun-cc-pVDZ. R_v = 3.6 Å for P and R_v = 4.9 Å for T.

The potential energy curves in Figure 2 have been obtained at a fixed vertical displacement, and this could lead to some misunderstandings. It is clear that for the sandwich structure at 3.6 Å the dimer shows a substantial repulsive contribution with a significant overlap, as also shown by the large penetration energy. Thus, it is expected that as the benzene molecules approach the sandwich structure the intermolecular distance will increase avoiding the large repulsion.[18, 20, 21] Similar considerations are valid for the T-shaped structure. Thus, the analysis carried out above has been repeated by using the values obtained for the most favourable vertical displacement for each slipped one. The best R_v for each R_s is obtained by interpolation of the total interaction energy, the rest of the contributions being obtained by interpolating the values at that optimum distance. The results are shown in Figure 3.

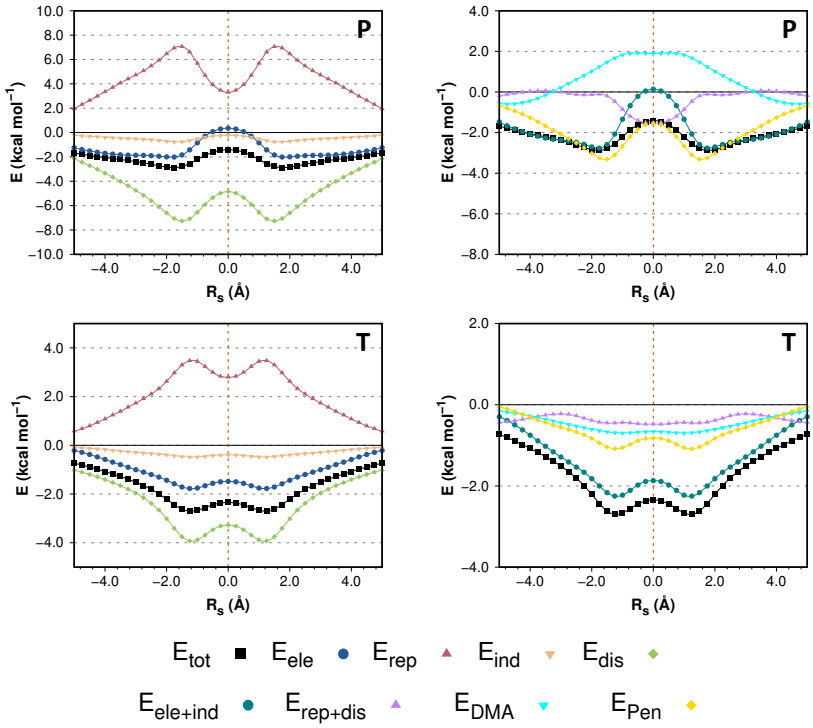

Figure 3. Potential energy curve for benzene dimer as obtained with SAPT0/jun-cc-pVDZ. R_v is the optimal value for each R_s.

The profiles for the total interaction energy shown in Figure 3 are not that different from the ones shown in Figure 2. The most noticeable change is that total interaction energies are lower in Figure 3 because now we are taking the best vertical displacement for each point. However, more significant differences are observed for the contributions to the interaction energy. In parallel structures both repulsion and dispersion contributions are not largest for the sandwich structure, because as R_s goes to zero, the rings depart from each other to avoid a large repulsion (R_v changes from around 3.5 Å

for the slipped parallel structure to around 3.9 Å for the sandwich one). Also, the total interaction energy now closely follows the changes in the electrostatic contribution.

The differences are more striking when comparing the grouped $E_{rep+dis}$ and $E_{ele+ind}$ contributions in Figure 3 (right). The overall behaviour is clearly controlled by the sum of induction and electrostatics, matching the total interaction energy. The combination of repulsion and dispersion favours the non-displaced structure and is almost negligible for any lateral displacement. Thus, the conclusions from Figure 3 are mostly contrary to those from Figure 2: it is the electrostatic contribution the one dictating the position of the minima, while the repulsion and dispersion contributions hardly affect to the interaction since they cancel each other to a large extent. In fact, it is as if dispersion makes the molecules to come closer against the repulsion wall, achieving a kind of draw, and therefore cancelling out and leading to a negligible overall contribution. With repulsion and dispersion mostly cancelling each other, the remaining contributions to the interaction energy are the ones dictating the most favourable arrangement.

Therefore, electrostatics dictates the preference for the parallel-displaced structure. However, this effect cannot be rationalised by means of a multipolar expansion since, as indicated in Figure 3 (right), the contribution from multipoles is mostly repulsive in P. However, electrostatic penetration shows a large contribution at displaced structures, and it is the main factor behind the preference for slipped minima. All other contributions do not favour the appearance of the slipped structure, which is only clearly favoured by the changes on electrostatic penetration. Thus, from the analysis above, it becomes clear that the preference of benzene dimer for the slipped-parallel structure is a consequence of the contribution of electrostatic penetration. The same conclusion can be reached from the analysis of the T-shaped structure. When optimised vertical displacements are employed, the total interaction energy curve closely follows changes in electrostatics. In this case, the combination of dispersion and repulsion is mildly attractive at any lateral displacement, while it is electrostatic penetration the contribution making the parallel-displaced structures more favourable. In the case of the T-shaped structure, the multipolar electrostatic energy is attractive, contributing to enhance the total electrostatic contribution, as induction does as well.

Summarizing, our results for benzene dimer show the importance of considering possible changes in vertical displacement in order to follow the minimum energy region of the potential energy surface. By doing so, our results clearly indicate that the preference for slipped structures in benzene dimer is dictated by electrostatics, and especially by the contribution of electrostatic penetration effects.

It could be argued that the observed behaviour is just a characteristic of the specific potential energy curves employed, obtained by displacing benzene along an axis passing through two *para* carbon atoms. Thus, interaction energies were also computed in a grid changing the three cartesian coordinates and putting the centre of the second benzene molecule on each point of the grid while keeping its relative orientation. The results can

be represented as 3D plots at a given vertical displacement or, as described above, using the optimum vertical displacement for each X-Y point. The results obtained are summarised in Figure 4 for the parallel benzene dimer, while the complete set of results is in the Supplementary Information (Figures S2 and S3).

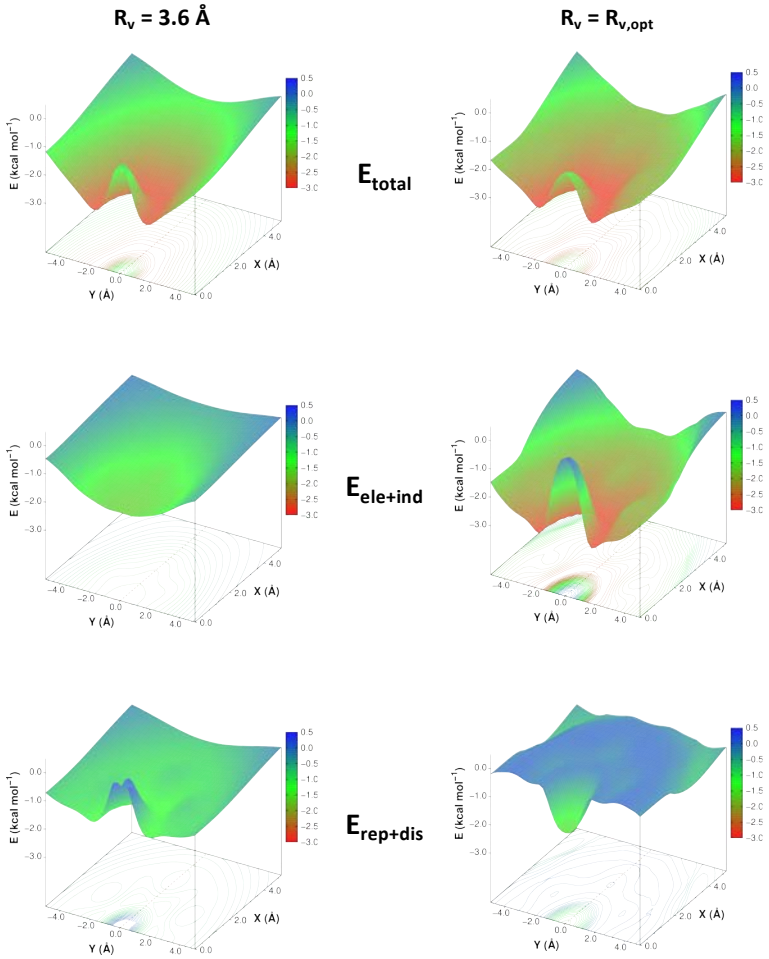

Figure 4. Energies obtained for the parallel benzene dimer. The Y axis passes through two *para* carbon atoms.

On the left column in Figure 4 the vertical displacement is kept at 3.6 Å as in the plots in Figure 2. The total interaction energy shows attractive regions corresponding to the slipped structures, over the C-C axis or slightly displaced from it. Considering the contributions from $E_{ele+ind}$ and $E_{rep+dis}$ there seems to be no correspondence between these contributions and the total interaction energy surface. At most, the $E_{ele+ind}$ term is quite isotropic leading to a minimum around the sandwich structure, while the $E_{rep+dis}$ term shows slightly attractive regions around the slipped structure, and a repulsive wall for the sandwich one.

The right column in Figure 4 shows the results obtained using the optimal vertical displacement for each point. The picture for the global interaction energy hardly

changes, its overall behaviour being mimicked by $E_{ele+ind}$, while the contributions coming from the $E_{rep+dis}$ term are much smaller and slightly repulsive in many points, hardly affecting the total interaction energy. The only region where the contribution of repulsion and dispersion is significant is precisely in the proximity of the sandwich structure, where it helps stabilising the dimer. Thus, our previous conclusions are confirmed; the slipped structures are favoured mainly by electrostatics, with penetration playing the greater part of the electrostatic contribution. The same conclusions are obtained for the T-shaped dimer as shown in the Supplementary Information (Figures S4 and S5).

The SAPT0 method employed does not describe intramonomer correlation effects, so it could be claimed that it could lead to wrong conclusions. Calculations have been also performed at the SAPT2+/aug-cc-pVDZ level[44] in benzene dimer to estimate the extent of intramonomer correlation terms. The results (Figure S7) indicate that there are slight differences, but the overall behaviour is the same as observed with SAPT0, showing the dominant role of electrostatics and electrostatic penetration in favouring displaced structures.

In any case, it is worth remembering that the partitioning of the total interaction energy is arbitrary to some extent. When analysing repulsion and dispersion individually, it is clear that dispersion shows a double well corresponding to the parallel-displaced structures (See Figures S3 and S5). Thus, dispersion, repulsion and electrostatic penetration behave in quite a similar way, with dispersion and penetration favouring the slipped structures while repulsion penalises them. The cancellation of repulsion and dispersion somewhat magnifies the role played by electrostatic penetration.

3.2. Benzene-X_{planar} dimers

The behaviour observed in the previous section could be just particular of benzene dimer and be different for other species. For this reason, a similar study has been carried out for heterodimers formed by benzene and other planar six-atom rings. The species have been chosen so they have no permanent dipole moment that could change electrostatics significantly, but include polar groups due to substitution which can affect the behaviour observed. Only the results obtained after interpolation of the most favourable structures are shown, while those obtained at a fixed distance are listed in the Supplementary Information (Figures S8 and S9).

Figure 5 shows the results obtained for parallel dimers. Starting with trifluorobenzene, it can be observed that now the curves are not symmetrical since the benzene molecule is displaced along an axis passing through opposite CH and CF groups, thus contacting with the CF group when R_s is positive and with the CH group when R_s is negative (See Figure 1). The structure slipped towards the CF group is favoured due to increased dispersion and electrostatics relative to the structure displaced to the CH group.

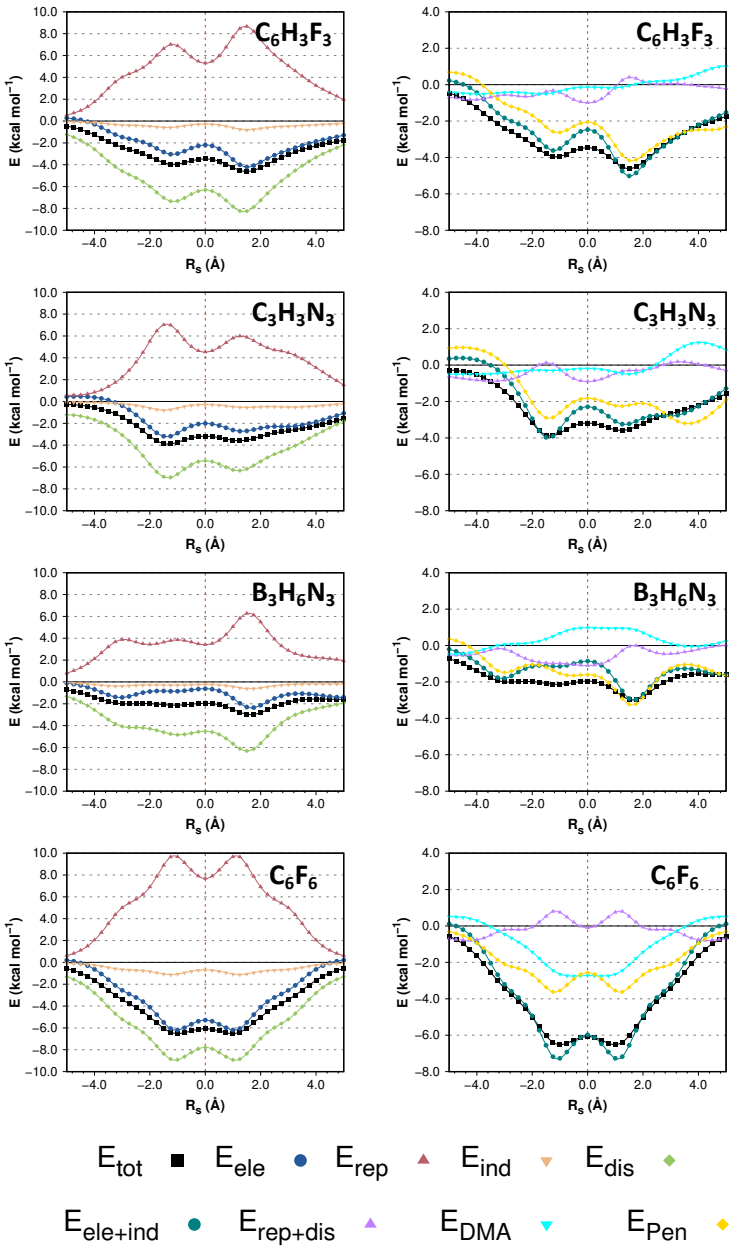

Figure 5. Potential energy curves for benzene P heterodimers as obtained with SAPT0/jun-cc-pVDZ. R_v is the optimal value for each R_s.

As in benzene dimer, the total interaction energy closely follows the trends indicated by the electrostatic contribution (if the curves are obtained at a fixed distance this does not happen as in benzene dimer, see Figures S8 and S9). Again, the slipped structures are favoured by electrostatics and dispersion. Analysing the grouped contributions it is observed that the combination of repulsion and dispersion is negligible, changing between roughly -1 to 0.5 kcal mol^{-1} for any of the displacements considered. On the other hand, the combination of electrostatics and induction changes more markedly, between 0 to -4 kcal mol^{-1}, almost reproducing the trends observed for the total interaction energies. Trifluorobenzene has a negligible quadrupole moment, so the

electrostatic interaction with benzene should be small following a simplistic quadrupole-quadrupole model. However, it is observed that the electrostatic interaction is even larger than the one observed in benzene dimer. Decomposing the electrostatic interaction on a multipolar term plus penetration energy, it is found that the multipolar contribution to the electrostatic interaction is really small, hardly reaching 1 kcal mol^{-1} for any displacement considered. It is the penetration contribution the one controlling the electrostatic term and, as it can be observed in Figure 5, it follows the same trend observed for the total interaction energy.

Similar conclusions can be reached in the case of the heterodimer formed by triazine and benzene. In this case, the most favourable structure is slipped to negative values, meaning stacking over the C-H group as in benzene, though the interaction energy profile is quite flat between -2 to 2 Å. The preference for displaced structures can again be related to larger contributions from dispersion and electrostatics. Considering $E_{ele+ind}$ and $E_{rep+dis}$, a cancellation between dispersion and repulsion is observed while electrostatics dictates the final trend found for the total interaction energy. As in trifluorobenzene, the electrostatic contribution mainly comes from penetration, with the multipolar term being small for most of the displacements considered. Only when the CH group is located over the nitrogen atom (around R_s = 4.0 Å), the multipolar electrostatic energy is somewhat repulsive leading to a minimum in the penetration energy.

The dimer formed by benzene and borazine shows similar characteristics overall. In this case there is a minimum corresponding to a structure with benzene slipped around 1.8 Å. In this structure benzene and borazine are parallel stacked so two carbon atoms are on top of two nitrogen atoms of borazine, while a CH group of benzene is over the centre of borazine and a BH group of borazine over the centre of benzene molecule. The other slipped structure, with the CH groups of benzene over two boron atoms, corresponding to a negative R_s, is less favourable. In any case, it can be observed that the most stable structure is favoured by an increased penetration energy.

Finally, the dimer formed by benzene and hexafluorobenzene is considered. The interaction energy profile is quite flat around the sandwich structure, but the most favourable arrangement is slightly displaced. As in the other dimers considered, the preference for this displaced structure is due to the contributions of dispersion and electrostatics. In this dimer, the electrostatic contribution is significantly larger than in the other dimers studied, reaching -6 kcal mol^{-1}. Once more, the total interaction energy closely follows the behaviour obtained for the electrostatic energy. $E_{ele+ind}$ and $E_{rep+dis}$ show the already well-known behaviour described above: repulsion and dispersion cancel each other so electrostatics dominates the shape of the interaction energy. It is worth noting that once again the profile obtained for the penetration energy mimics the one observed for the total interaction energy. The main difference with previous cases is that in this dimer the multipolar contribution is significant and attractive, especially

around the sandwich structure, enhancing the final contribution of the electrostatic energy. In any case, the multipolar electrostatic energy is mostly flat between -2 to 2 Å, so it has no effect on the preference for slipped structures.

Regarding T-shaped structures, the results obtained are shown in Figure 6. Benzene is displaced with two C-H groups pointing towards the ring of the other species considered in this work as represented in Figure 1. In the complex with trifluorobenzene the most favourable structure is displaced toward the C-F group, mainly because of favourable contributions from electrostatics and dispersion. When the different contributions are grouped into electrostatic and van der Waals terms, it is observed that electrostatics controls the shape of the total interaction energy curve. As in previous cases, electrostatics is mostly coming from penetration, with the multipolar term being slightly negative when the CH groups points toward the fluorine atom.

The benzene-triazine dimer shows the most complex behaviour, with two minima corresponding to a slightly displaced benzene and to a much more displaced one (around R_s = 5 Å, see figure associated to Table S1). It can be clearly observed that the first minimum is similar to the ones observed for benzene dimer and trifluorobenzene-benzene dimer, being favoured by dispersion and electrostatics, while the second structure is mostly favoured by electrostatics. This is more clearly seen when grouping the contributions. $E_{rep+dis}$ is small and attractive for most of the displaced structures, except when reaching values of R_s larger the 3 Å, where the contribution becomes repulsive. On the other hand, electrostatics becomes largely attractive in the same region. While electrostatics is mostly controlled by penetration, in this second structure the contribution from the multipolar term is even larger. All these effects occur because when the lateral displacement is larger than 3 Å, one of the CH groups points directly towards the nitrogen lone pair. As a consequence, the vertical displacement decreases to favour this CH···N contact, leading to an increase of repulsion and dispersion as well as penetration. The large contribution from the multipole expansion reflects the electrostatic favourable contact between the nitrogen lone pair and the hydrogen atom in the CH group.

Compared to triazine, the dimer formed with borazine behaves more typically, with electrostatics controlling the behaviour of the total interaction energy. In the dimer formed with hexafluorobenzene, the most striking effect is the significantly repulsive electrostatic term obtained from the multipole analysis, as a consequence of positively charged hydrogens pointing to the also positive ring. Thus, the large penetration energy (matching again the changes in total energy) is partially cancelled out by the multipolar term.

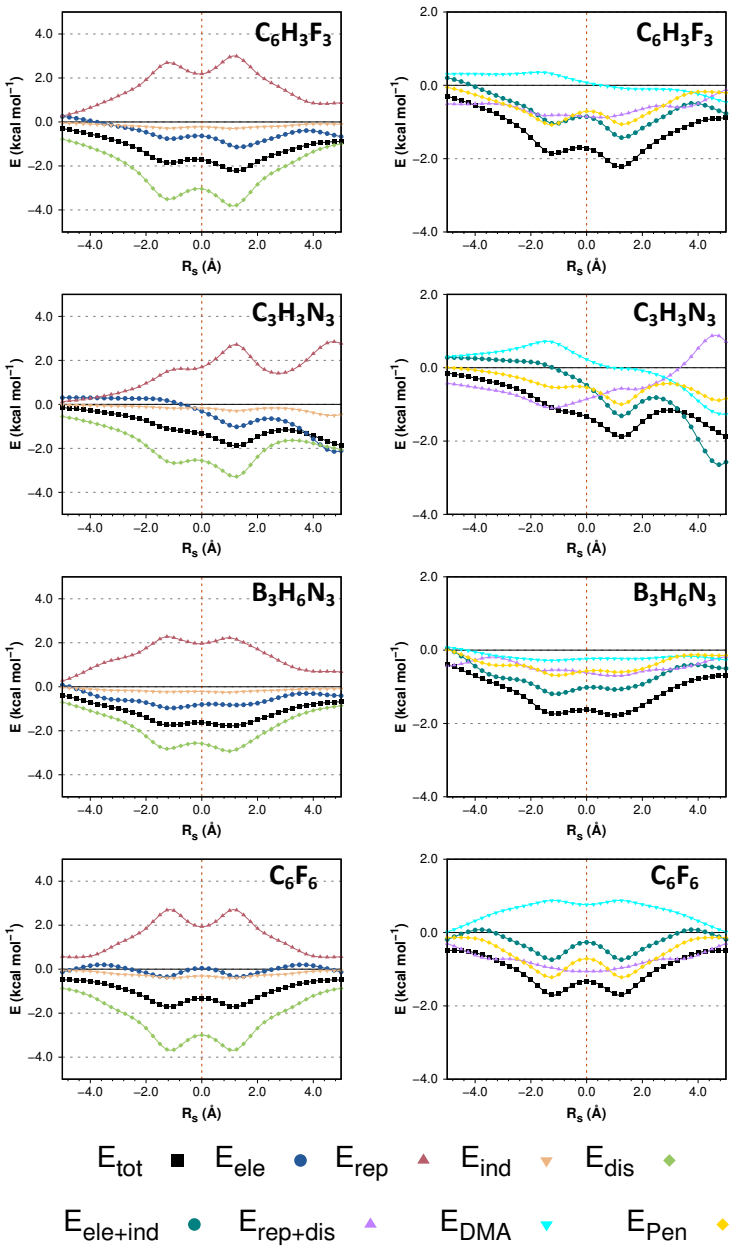

Figure 6. Potential energy curve for benzene T heterodimers as obtained with SAPT0/jun-cc-pVDZ. R_v is the optimal value for each R_s.

Therefore, in all dimers considered the terms contributing the most to the stability of the complex are electrostatics and, specially, dispersion. However, since dispersion is largely cancelled by repulsion, the final interaction energy profile follows the changes in electrostatic energy, which is the term finally deciding the preference for displaced structures. A great part of the electrostatic contributions is due to electrostatic penetration, so the behaviour cannot be rationalized in terms of the multipoles of the interacting molecules. The contribution of penetration to the interaction energy amounts between 17 to 33 % of the total stabilizing contributions in P dimers and between 15 to 35 % in T dimers, with an average contribution of 23% of the total

stabilizing contributions at the minima (see Table S1). Thus, electrostatic penetration energy not only dictates the total interaction energy profile, but also makes an important contribution of around 25% of the total stabilization of the dimer.

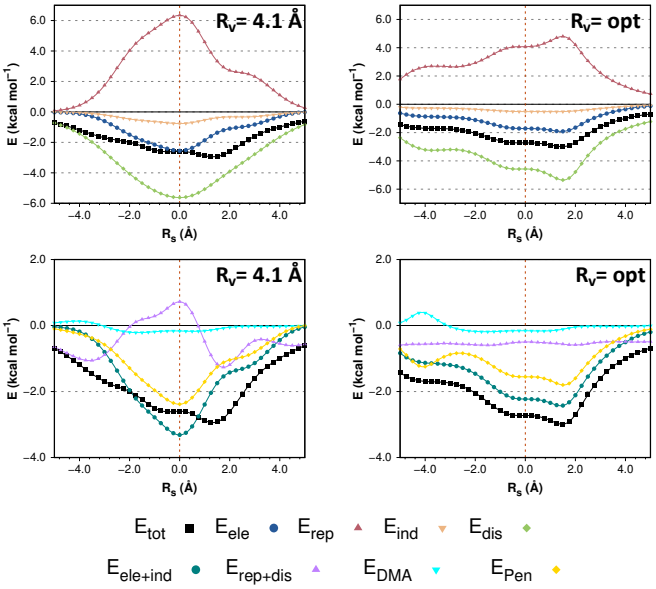

Figure 7. Potential energy curves for benzene-cyclohexane dimer as obtained with SAPT0/jun-cc-pVDZ.

3.3. Benzene-Cyclohexane dimer

The stacking interaction involving aliphatic species has recently drawn attention, because it can be of similar intensity as the stacking between aromatic species. The interaction in cyclohexane dimer is slightly weaker than the one observed in benzene dimer, while the interaction between benzene and cyclohexane is even stronger.[10, 13, 19, 50] However, it has also been shown that as the aliphatic system increases in size the interaction energy increases at a slower rate than in aromatic analogues.[7, 10, 11]

Figure 7 shows the results obtained when sliding a benzene molecule over cyclohexane. At a fixed vertical distance of 4.1 Å, electrostatics and dispersion favour a totally stacked dimer, while there seems that repulsion leads to a displaced structure. However, it is much harder to find a clear relation between any of the contributions and the behaviour obtained for the total interaction energy changes. When the optimized vertical displacement is employed, the behaviour observed is compatible with the one discussed in previous sections; the trends in total interaction energy are clearly matched by changes in electrostatics. Once $E_{rep+dis}$ and $E_{ele+ind}$ contributions are considered it becomes clear that the changes observed for the total interaction energy are due to changes in electrostatic energy, mostly coming from electrostatic penetration.

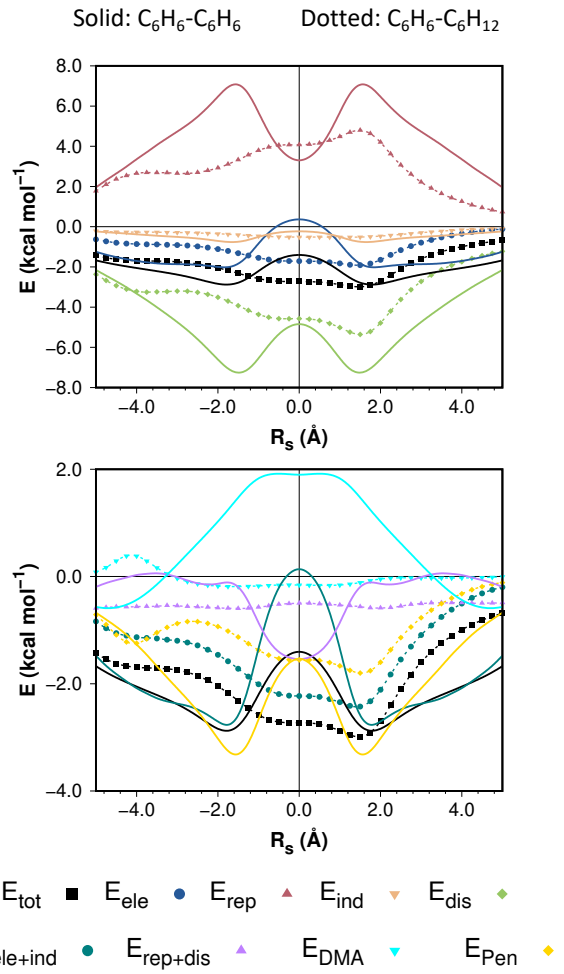

Figure 8. Comparison between benzene dimer (solid) and benzene-cyclohexane dimer (dotted).

Figure 8 compares the changes in interaction energy for benzene-benzene and cyclohexane-benzene dimers. The heterodimer is more stable at small lateral displacements (below 2 Å, roughly) while benzene dimer becomes more stable at large lateral displacements. Ninkovic et al. have suggested that the stability observed in many aromatic parallel-slipped dimers is related to a larger electrostatic contribution at long range when compared to aliphatic species.[19] As observed in Figure 8, for R_v > 2 Å, the contribution coming from the electrostatic terms $E_{ele+ind}$ is smaller in cyclohexane-benzene dimer. Since the contribution from the multipolar electrostatic interaction is almost zero in the heterodimer, the electrostatic contribution mostly comes from penetration. The contribution from penetration in benzene dimer is even larger because the multipolar contribution is clearly repulsive for lateral displacements below 3.5 Å.

In agreement with Ninkovic et al.,[19] slipped benzene dimers still show significant interaction energies due to larger electrostatics contributions that arise from electrostatic penetration. Besides, at larger lateral displacements, where the

penetration effects are similar in benzene-benzene and cyclohexane-benzene dimers, there is a significant contribution from the multipolar interaction in benzene dimer while its contribution is negligible in the heterodimer. Therefore, the electrostatic contribution is larger in slipped benzene dimer due to larger penetration effects or, when penetration effects are of similar magnitude, due to favourable multipole-multipole interactions. The behaviour is somewhat different when comparing the cyclohexane-benzene dimer with the T-shaped benzene dimer, both exhibiting similar electrostatic contributions (see Figure S12). Due to the larger intermolecular distances in the T-shaped dimer, the contribution of electrostatic penetration decays compared to that observed in the parallel benzene dimer, becoming even smaller than the one observed in cyclohexane-benzene dimer.

4. Conclusions

The nature of the interaction in benzene-containing dimers has been thoroughly analysed by using SAPT0 calculations. In benzene dimer, dispersion and repulsion are the largest contributions to the interaction energy; thus, the observed behaviour could be roughly interpreted as a balance between them, with no role played by electrostatics. However, it turns out that this is a consequence of a partial analysis resulting from keeping a fixed intermolecular distance. When the results are analysed considering the optimal separation between aromatic rings, the behaviour is totally different, with electrostatics controlling the overall trends observed for the total interaction energy.

The picture that emerges is that dispersion and repulsion mostly cancel out at the most favourable intermolecular separations, so the global changes in the interaction energy are controlled by electrostatics. Thus, the geometry of the most favourable dimer structures is mainly dictated by the electrostatic interaction and, more specifically, by electrostatic penetration.

The observed behaviour is not exclusive of benzene dimer, and it is also observed for a series of heterodimers formed by benzene and substituted benzene rings, as well as in cyclohexane-benzene dimer. In all cases, the global changes in the interaction energy are controlled by the electrostatic contribution, and more specifically by the electrostatic penetration energy. The main difference between benzene dimer and cyclohexane-benzene dimer resides on the larger range of the electrostatic interaction between benzene molecules.

In summary, even though the electrostatic contribution to the interaction energy is not the largest contribution to the global stability in complexes formed by benzene, it is the one controlling the final trends on the interaction energy at optimal intermolecular separations. At these optimal separations, the contributions from repulsion and dispersion cancel out to a large extent, while the short interatomic distances lead to significant overlap and to the breaking down of the multipolar description of the

electrostatic energy. Thus, multipoles should not be employed to rationalize the behaviour observed in this kind of complexes, because the electrostatic energy mostly corresponds to electrostatic penetration. In consequence, models trying to represent the behaviour of these systems should include an appropriate description of penetration effects, maybe by including specific terms or by absorbing the contribution of penetration in properly modified van der Waals potentials.

Acknowledgments

The authors thank the financial support from the Consellería de Cultura, Educación e Ordenación Universitaria e da Consellería de Economía, Emprego e Industria (Axuda para Consolidación e Estruturación de unidades de investigación competitivas do Sistema Universitario de Galicia, Xunta de Galicia ED431C 2021/40). The authors also want to express their gratitude to the CESGA (Centro de Supercomputación de Galicia) for the use of their computers.

Conflicts of interest

There are no conflicts to declare

References

1. E. A. Meyer, R. K. Castellano and F. Diederich, *Angew. Chem. Int. Ed.*, 2003, **42**, 1210-1250.
2. L. M. Salonen, M. Ellermann and F. Diederich, *Angew. Chem. Int. Ed.*, 2011, **50**, 4808-4842.
3. E. M. Pérez and N. Martín, *Chem. Soc. Rev.*, 2015, **44**, 6425-6433.
4. D. W. Johnson and F. Hof, *Aromatic Interactions: Frontiers in Knowledge and Application*, The Royal Society of Chemistry, 2017.
5. T. Akasaka, A. Osuka, S. Fukuzumi, H. Kandori and Y. Aso, *Chemical Science of π-Electron Systems*, Springer Japan, Tokyo, 2015.
6. S. Grimme, *Angew. Chem. Int. Ed.*, 2008, **47**, 3430-3434.
7. S. Ehrlich, J. Moellmann and S. Grimme, *Acc. Chem. Res.*, 2013, **46**, 916-926.
8. K. S. Kim, S. Karthikeyan and N. J. Singh, *J. Chem. Theory Comput.*, 2011, **7**, 3471-3477.
9. T. Janowski and P. Pulay, *J. Am. Chem. Soc.*, 2012, **134**, 17520-17525.
10. M. Alonso, T. Woller, F. J. Martín-Martínez, J. Contreras-García, P. Geerlings and F. DeProft, *Chem. Eur. J.*, 2014, **20**, 4931-4941.
11. E. M. Cabaleiro-Lago and J. Rodríguez-Otero, *ACS Omega*, 2018, **3**, 9348-9359.
12. C. R. Martinez and B. L. Iverson, *Chem. Sci.*, 2012, **3**, 2191-2201.
13. E. M. Cabaleiro-Lago and J. Rodríguez-Otero, *ChemistrySelect*, 2017, **2**, 5157-5166.
14. R. Podeszwa, R. Bukowski and K. Szalewicz, *J. Phys. Chem. A*, 2006, **110**, 10345-10354.
15. S. Tsuzuki, K. Honda, T. Uchimaru, M. Mikami and K. Tanabe, *J. Am. Chem. Soc.*, 2002, **124**, 104-112.
16. E. M. Cabaleiro-Lago, J. Rodríguez-Otero and S. A. Vázquez, *Phys. Chem. Chem. Phys.*, 2020, **22**, 12068-12081.
17. S. A. Arnstein and C. D. Sherrill, *Phys. Chem. Chem. Phys.*, 2008, **10**, 2646-2655.
18. M. O. Sinnokrot, E. F. Valeev and C. D. Sherrill, *J. Am. Chem. Soc.*, 2002, **124**, 10887-10893.
19. D. B. Ninković, J. P. Blagojević Filipović, M. B. Hall, E. N. Brothers and S. D. Zarić, *ACS Central Science*, 2020, **6**, 420-425.
20. K. Min Seung, C. Lee Eun, M. Lee Han, Y. Kim Dong, D. Kim and S. Kim Kwang, *J. Comput. Chem.*, 2008, **29**, 1208-1221.
21. M. Pitoňák, P. Neogrády, J. Řezáč, P. Jurečka, M. Urban and P. Hobza, *J. Chem. Theory Comput.*, 2008, **4**, 1829-1834.
22. C. A. Hunter, K. R. Lawson, J. Perkins and C. J. Urch, *J. Chem. Soc. Perkin Trans. 2*, 2001, 651-669.
23. C. A. Hunter and J. K. M. Sanders, *J. Am. Chem. Soc.*, 1990, **112**, 5525-5534.
24. M. O. Sinnokrot and C. D. Sherrill, *J. Am. Chem. Soc.*, 2004, **126**, 7690-7697.
25. M. O. Sinnokrot and C. D. Sherrill, *J. Phys. Chem. A*, 2003, **107**, 8377-8379.
26. A. L. Ringer and C. D. Sherrill, *J. Am. Chem. Soc.*, 2009, **131**, 4574-4575.
27. S. E. Wheeler and K. N. Houk, *J. Am. Chem. Soc.*, 2008, **130**, 10854-10855.
28. S. E. Wheeler, *J. Am. Chem. Soc.*, 2011, **133**, 10262-10274.
29. S. E. Wheeler, *Acc. Chem. Res.*, 2013, **46**, 1029-1038.
30. R. K. Raju, J. W. G. Bloom, Y. An and S. E. Wheeler, *ChemPhysChem*, 2011, **12**, 3116-3130.

31. K. Carter-Fenk and J. M. Herbert, *Chem. Sci.*, 2020, **11**, 6758-6765.
32. K. Carter-Fenk and J. M. Herbert, *Phys. Chem. Chem. Phys.*, 2020, **22**, 24870-24886.
33. S. M. Ryno, C. Risko and J.-L. Brédas, *Chem. Mater.*, 2016, **28**, 3990-4000.
34. A. J. Stone, *The theory of intermolecular forces*, Oxford University Press, Oxford, 2013.
35. G. Gryn'ova and C. Corminboeuf, *Beilstein J. Org. Chem.*, 2018, **14**, 1482–1490.
36. J. M. Herbert, *J. Phys. Chem. A*, 2021, **125**, 7125-7137.
37. M. P. Hodges, A. J. Stone and E. C. Lago, *J. Phys. Chem. A*, 1998, **102**, 2455-2465.
38. E. M. Cabaleiro-Lago and M. A. Rios, *J. Chem. Phys.*, 1999, **110**, 6782-6791.
39. F. Jiménez-Grávalos and D. Suárez, *J. Chem. Theory Comput.*, 2021, **17**, 4981-4995.
40. J. A. Rackers, Q. Wang, C. Liu, J.-P. Piquemal, P. Ren and J. W. Ponder, *Phys. Chem. Chem. Phys.*, 2017, **19**, 276-291.
41. A. Katrusiak, M. Podsiadło and A. Budzianowski, *Crystal Growth & Design*, 2010, **10**, 3461-3465.
42. E. G. Hohenstein and C. D. Sherrill, *WIREs Comput. Mol. Sci.*, 2012, **2**, 304-326.
43. K. Patkowski, *WIREs Comput. Mol. Sci.*, 2020, **10**, e1452.
44. T. M. Parker, L. A. Burns, R. M. Parrish, A. Ryno, G and C. D. Sherrill, *J. Chem. Phys.*, 2014, **140**, 094106.
45. A. J. Stone, *J. Chem. Theory Comput.*, 2005, **1**, 1128-1132.
46. *TURBOMOLE V6.3 2011, a development of University of Karlsruhe and Forschungszentrum Karlsruhe GmbH, 1989-2007, TURBOMOLE GmbH, since 2007; available from* http://www.turbomole.com.
47. A. J. Stone, A. Dullweber, O. Engkvist, E. Fraschini, M. P. Hodges, A. W. Meredith, D. R. Nutt, P. L. A. Popelier and D. J. Wales, Orient: a program for studying interactions between molecules, version 5.0. University of Cambridge, 2018.
48. M. J. Frisch, G. W. Trucks, H. B. Schlegel, G. E. Scuseria, M. A. Robb, J. R. Cheeseman, G. Scalmani, V. Barone, G. A. Petersson, H. Nakatsuji, X. Li, M. Caricato, A. V. Marenich, J. Bloino, B. G. Janesko, R. Gomperts, B. Mennucci, H. P. Hratchian, J. V. Ortiz, A. F. Izmaylov, J. L. Sonnenberg, Williams, F. Ding, F. Lipparini, F. Egidi, J. Goings, B. Peng, A. Petrone, T. Henderson, D. Ranasinghe, V. G. Zakrzewski, J. Gao, N. Rega, G. Zheng, W. Liang, M. Hada, M. Ehara, K. Toyota, R. Fukuda, J. Hasegawa, M. Ishida, T. Nakajima, Y. Honda, O. Kitao, H. Nakai, T. Vreven, K. Throssell, J. A. Montgomery Jr., J. E. Peralta, F. Ogliaro, M. J. Bearpark, J. J. Heyd, E. N. Brothers, K. N. Kudin, V. N. Staroverov, T. A. Keith, R. Kobayashi, J. Normand, K. Raghavachari, A. P. Rendell, J. C. Burant, S. S. Iyengar, J. Tomasi, M. Cossi, J. M. Millam, M. Klene, C. Adamo, R. Cammi, J. W. Ochterski, R. L. Martin, K. Morokuma, O. Farkas, J. B. Foresman and D. J. Fox, Gaussian Inc., Wallingford CT, 2016.
49. R. M. Parrish, L. A. Burns, D. G. A. Smith, A. C. Simmonett, A. E. DePrince, E. G. Hohenstein, U. Bozkaya, A. Y. Sokolov, R. Di Remigio, R. M. Richard, J. F. Gonthier, A. M. James, H. R. McAlexander, A. Kumar, M. Saitow, X. Wang, B. P. Pritchard, P. Verma, H. F. Schaefer, K. Patkowski, R. A. King, E. F. Valeev, F. A. Evangelista, J. M. Turney, T. D. Crawford and C. D. Sherrill, *J. Chem. Theory Comput.*, 2017, **13**, 3185-3197.

50. D. B. Ninkovic, D. Z. Vojislavljevic-Vasilev, V. B. Medakovic, M. B. Hall, E. N. Brothers and S. D. Zaric, *Phys. Chem. Chem. Phys.*, 2016, **18**, 25791-25795.

TOC

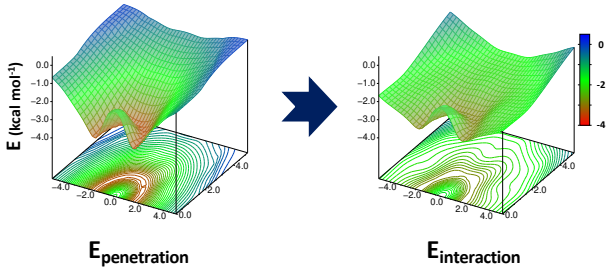

Electrostatic penetration shapes the total interaction energy in aromatic dimers